

# Bifunctional Behavior of Bulk $\text{MoO}_x\text{N}_y$ and Nitrated Supported NiMo Catalyst in Hydrodenitrogenation of Indole

K. Miga,\* K. Stanczyk,\* C. Sayag,† D. Brodzki,† and G. Djéga-Mariadassou†<sup>1</sup>

\*Institute of Coal Chemistry, Polish Academy of Sciences, ul. Sowinskiego 5, 44-102 Gliwice, Poland; and †Université P. et M. Curie, Laboratoire Réactivité de Surface, CNRS-UMR 7609, 4 Place Jussieu, Casier 178, 75252 Paris Cedex 05, France

Received July 16, 1998; revised October 22, 1998; accepted December 10, 1998

Oxynitrides of early transition metals are bifunctional catalysts (metallic and acidic sites) active in hydrodenitrogenation (HDN). The HDN of indole was used as a molecular probe reaction to study the metallic and acidic properties of the dual sites on oxynitrides. The behavior of those sites was found to be different from that of supported and sulfided NiMo. The reaction was conducted at low partial pressure of  $\text{H}_2\text{S}$  over both a bulk  $\text{MoO}_x\text{N}_y$  and a supported NiMo catalyst, nitrated before the reaction. Under high hydrogen pressure, HDN of indole was shown to occur with or without prior hydrogenation of the aromatic ring of orthoethylaniline, leading to either ethylbenzene or ethylcyclohexane. Secondary reactions, such as the joining of heterocyclic rings (leading to 1-4 tetrahydroquinoline) and dimerization, were found to occur as a result of the presence of acidic sites. Hydrogenolysis of the lateral chain of orthoethylaniline was also observed. © 1999 Academic Press

**Key Words:** molybdenum oxynitride; bulk; supported; high pressure HDN.

## 1. INTRODUCTION

The main bulk or surface characteristics of nitrides and carbides of early transition metals will be described again in order to clarify the main concepts used in this work. Insertion of nitrogen or carbon into the lattice of early transition metals (groups 4 to 6) is now known to transfer some of the properties of precious metals to these transition metals. Carbon, in particular, causes them to hydrogenate stronger than does the insertion of nitrogen (1). Another important feature is the ability of these materials to adapt their own chemical composition to that of the feed during reactions. Carbon, nitrogen, and oxygen atoms can then exchange, leading to the real catalytically active phase. A fundamental question remains: can sulfur or phosphorus atoms also be inserted into the nitride or carbide lattice?

After synthesis, nitrides or carbides are pyrophoric, and a passivation step is required to prevent the bulk oxidation of these materials on exposure to air. A treatment with 1 vol%  $\text{O}_2$ /helium at room temperature leads to an oxy-

gen surface monolayer. Subsequently, oxygen atoms can react with hydrogen atoms in the bulk during the nitridation or carburization processes. Hydrogen atoms can diffuse from the bulk to the surface and lead to OH surface groups. Several fundamental studies on tungsten carbides (Ribeiro *et al.* (2) and Muller *et al.* (3)) and on oxynitrides (Sellem *et al.* (4)) recently demonstrated the existence of surface Brønsted acidity in the isomerization of alkanes.

As a result, two types of sites exist on the surface of nitrides or carbides prepared at high temperature after exposure to oxygen: metallic sites (early transition metal atoms modified by C and/or nitrogen) and acidic sites (Brønsted groups). Lewis sites, due to low oxidation states of the transition metal, cannot be excluded. Therefore, nitrides and carbides of transition metals prepared at high temperature are *bifunctional*. Oxygen-containing nitrides and carbides are called “oxynitrides” ( $\text{MeO}_x\text{N}_y$ ) and “oxycarbides” ( $\text{MeO}_x\text{C}_y$ ) respectively.

In the case of molybdenum carbides, there is some confusion between the high temperature carbides, prepared according to Volpe and Boudart (5), and the low temperature molybdenum carbides prepared by Ledoux and co-workers (6). The latter materials are prepared by inserting carbon into the lattice of molybdenum oxide and were found to be monofunctional catalysts in alkane isomerization (6).

A characteristic of high temperature nitrides and carbides is that Brønsted groups and transition metal atoms can exist side by side on the surface of the solid. The concept of a “dual site” led us to propose a model for  $\text{MoO}_x\text{N}_y$  (7) (Fig. 1).  $\text{MoO}_x\text{N}_y$ , prepared at high temperature, presents a NaCl-like cubic structure. The fcc sublattice of molybdenum atoms defines octahedral sites located either in the center or on the edges of the cube, where N, C, or O atoms can be inserted. A dual site can be defined by a metallic center such as a Mo atom, electronically modified by N or C atoms, and an acidic site (Brønsted group). Vacancies can exist in the sublattice of molybdenum, as shown by Gouin *et al.* (8). Therefore, these materials are nonstoichiometric, but counting metallic sites can be done by specific CO chemisorption under well-defined conditions (9).

<sup>1</sup> To whom correspondence should be addressed.

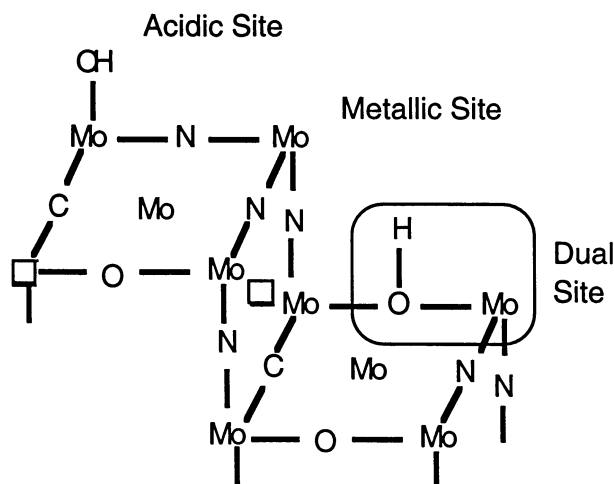


FIG. 1. Acidic site (OH group), metallic site (Mo), and dual site model for  $\text{MoO}_x\text{N}_y$ .

One aim of the present work was to study the effect of surface acidity on the product distribution of indole reactions during HDN of indole. To study the effect of the strength and number of Brønsted groups, strong acidic sites are created by supporting  $\text{MoO}_x\text{N}_y$  on a mixed  $[\text{Al}_2\text{O}_3/\text{H-ZSM-5}]$  support.

A second aim deals with the study of the reaction pathways of HDN of indole and secondary reactions occurring via acidic centers.

## 2. EXPERIMENTAL

### 2.1. Catalysts

Two kinds of nitrides were prepared: a bulk  $\text{MoO}_x\text{N}_y$  and a nitrated NiMo supported catalyst referred to as 76aN.

**Bulk  $\text{MoO}_x\text{N}_y$ .** Molybdenum trioxide (Janssen-Chimica) was used as the precursor of  $\text{MoO}_x\text{N}_y$ . Nitridation was carried out according to the procedure of Volpe and Boudart (5). Precursors (about 2 g) were placed in a quartz reactor and nitrated in pure flowing  $\text{NH}_3$  (VHSV =  $37,500 \text{ h}^{-1}$ ). Temperature was increased in three steps, first quickly from 293 to 633 K ( $17 \text{ K min}^{-1}$ ), then more slowly from 633 to 733 K ( $33 \text{ K h}^{-1}$ ), and from 733 to 973 K ( $100 \text{ K h}^{-1}$ ). The temperature was held at 973 K for 3 h. The system was then cooled to room temperature in flowing  $\text{NH}_3$  and flushed in helium for 0.5 h. The sample was passivated by flowing 1 vol%  $\text{O}_2$  in He for 1 h, before exposure to air. The X-ray diffraction pattern of the bulk molybdenum oxynitride showed the characteristic lines of  $\gamma\text{-Mo}_2\text{N}$ . Elemental chemical analysis indicated that the material contained 7 wt% oxygen after passivation. Its total specific surface area was  $130 \text{ m}^2 \cdot \text{g}^{-1}$ , and its pore volume was  $0.17 \text{ cm}^3 \cdot \text{g}^{-1}$ .

**Supported  $\text{MoO}_x\text{N}_y$ .** The precursor of 76aN was a Polish NiMo catalyst referred to as 76a from the Institute of Petroleum and Coal Chemistry, Wroclaw. In recent years, this catalyst has been generally used for hydrotreating coal-derived fuels after sulfidation. With such a feedstock, no limitation of external diffusion was observed. This precursor was used in the present study for two reasons: (i) it was of interest to nitride, instead of sulfide, the oxidic form of this supported catalyst to determine whether the nitridation process can be extrapolated to already existing hydrotreating catalyst precursors, and (ii) it permitted stronger acidity of the molybdenum nitride-supported catalyst. The precursor consisted of 4 wt% NiO + 16 wt%  $\text{MoO}_3$  supported on modified alumina ( $\text{Al}_2\text{O}_3 + 20 \text{ wt\%}$  of NiH-ZSM-5). The nickel-exchanged form of H-ZSM-5 was obtained according to the following steps:



The XRD pattern of 76aN showed that the crystallinity of the zeolite was preserved after nitridation, as observed previously with the EMT zeolite (10). The total specific surface area of 76aN was  $205 \text{ m}^2 \cdot \text{g}^{-1}$ , and its pore volume was  $0.36 \text{ cm}^3 \cdot \text{g}^{-1}$ .

According to published data on bulk (2, 5, 11) and supported (10, 11) oxynitrides, both bulk molybdenum oxynitrides and nitrated supported commercial NiMo catalysts were black, a characteristic of nitrated materials.

Temperature-programmed desorption (TPD) in the vacuum of preadsorbed ammonia at 370 K showed that 76a and 76aN materials mainly exposed medium strength acid sites (desorption temperature of  $\text{NH}_3$  between 570 and 720 K). No drastic difference was observed between the  $\text{NH}_3$  TPD profiles of 76a and 76aN, indicating that acidity was preserved after nitridation. The  $\text{MoO}_x\text{N}_y$  acidic sites were mainly weak, as shown by the lower temperature TPD peaks of ammonia. This was also observed by Nagai *et al.* (12).

### 2.2. Catalytic Tests

Runs were performed in a high-pressure flow reactor, equipped with a Deoxo device for hydrogen purification (13). The main part of the apparatus is a fixed bed steel reactor containing  $2 \text{ cm}^3$  of catalyst. The initial liquid feed (cyclohexane or indole in cyclohexane) was provided by a high-pressure pump.

### 2.3. Catalytic Runs

All runs were conducted in flowing hydrogen at high pressure (9.0 MPa) in the presence of 70 ppm  $\text{H}_2\text{S}$  without any prereduction of the catalysts. The liquid hourly space velocity of the feed was  $2 \text{ h}^{-1}$ , with a volume ratio between hydrogen and the feed equal to 1000:1. The feed was a

solution of 2 wt% indole (Fluka, purity > 99%) in cyclohexane. The catalyst volume was always 2  $\text{cm}^3$  (76aN, 2.1 g and  $\text{MoO}_x\text{N}_y$ , 2.7 g).

The temperature profile of each run as well as the changes in the feed during the runs were as follows. A run cycle consisted of five 12-h periods (60 h) and of two 1-h periods while the temperature increased. Each cycle started and ended with 12-h periods of blank feed when only cyclohexane (CH) was supplied. The liquid product was collected in a high-pressure separator. Sampling was performed every 2 h. After the initial temperature increase, steady state was achieved after 2 h. Analytical data of the two last samplings were taken into account for each period. Both catalysts (bulk and supported) were subjected to the above procedure.

### 3. RESULTS AND DISCUSSION

#### 3.1. Reaction Network of HDN of Indole

Figure 2 presents the reaction network of HDN of indole according to Abe and Bell (14). The acronyms are also listed. Two main routes can be defined for the removal of the nitrogen atom from indole. The first, route 1, leads to ethylbenzene (EB) through orthoethylaniline (OEA), without saturation of the aromatic ring of OEA. This route is most desirable, because it consumes less hydrogen.

The second route (Fig. 2, route 2), observed in the presence of sulfided commercial catalysts, goes through hexahydroindole (HHI) and orthoethylcyclohexylamine (OECHA) to ethylcyclohexane (ECH) or, with saturation of the aromatic ring of OEA, to OECHA, prior to the removal of the nitrogen atom as  $\text{NH}_3$ . Two of the reactions involved in these HDN routes are hydrogenation and hydrogenolysis of C–N bonds. Both can be considered characteristic of the metallic function of the catalyst. Whether hydrogenolysis involves an acidic function remains an open

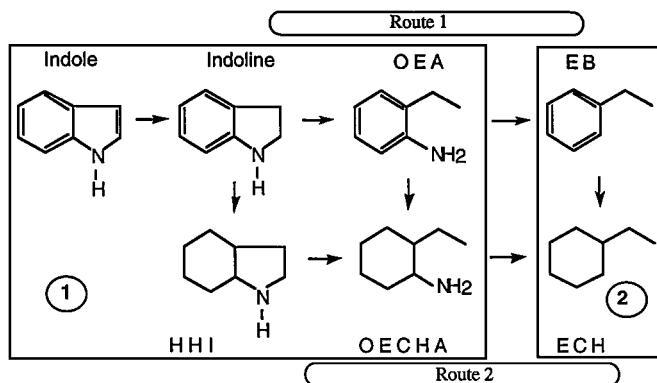


FIG. 2. General scheme for HDN of indole at 630 K and 9.1 MPa, going beyond Abe and Bell's proposal (14). (1) Nitrogen-containing compounds. HHI, hexahydroindoline; OEA, orthoethylaniline; OECHA, orthoethylcyclohexylamine. (2) EB, ethylbenzene; ECH, ethylcyclohexane.

TABLE 1

Product Distribution (mol%) Formed at 630 K, 9.1 MPa under Standard Conditions (1 wt% indole in cyclohexane, 70 ppm  $\text{H}_2\text{S}$ ) on Nonnitrided 76a

Catalyst	76a
Indole and N-containing compounds	
Indole	0.8
Indoline	0
Orthoethylaniline	0
Orthomethylaniline	0
Aniline	0
C4-aniline	0
Sum	0.8
Indole HDN products	
Ethylcyclohexane	0
Ethylcyclohexene	0
Ethylbenzene	0
C4-cyclohexane	0
C4-benzene	0
Sum	0
Solvent	
Cyclohexane	90.6
Solvent products	
Methylcyclohexane	0.5
Ethylcyclohexane	0.9
Sum	1.4
Solvent isomers	
Methylcyclopentane	6.9
Cyclopentane	1.1
Sum	8.0
Total	100.8

question. As will be shown, route 1 of HDN of indole is far from negligible on bulk  $\text{MoO}_x\text{N}_y$  and 76aN, even at high hydrogen pressure [9.1 MPa].

#### 3.2. Blank Runs

Nickel in 76a is present as Ni species associated with molybdenum as well as Ni exchanged in H-ZSM-5. In order to rule out possible HDN activity of Ni species in 76a in the presence of low  $\text{H}_2\text{S}$  pressure, without prior nitridation (not nitrided molybdenum being considered as inactive in HDN), blank runs were made at 630 K under our standard conditions (especially in the presence of 9.0 MPa  $\text{H}_2$  and 70 ppm  $\text{H}_2\text{S}$ ). Table 1 reports the product distribution of the corresponding runs. It clearly shows that there is no HDN of indole and only some alkylation or isomerization of the solvent.

Ni in the presence of sulfur, at high temperature and high pressure, is easily sulfided and becomes inactive (15–17).

#### 3.3. HDN of Indole over $\text{MoO}_x\text{N}_y$ at 600 K

Table 2 shows that 93.3 mol% indole is transformed at 600 K, but 65.7 mol% of the products still N-contain

TABLE 2

**Distribution of Reaction Products and Intermediates (in mol%) Formed at 600 K at 9.1 MPa over MoO<sub>x</sub>N<sub>y</sub> and 76aN Catalysts**

Catalysts	MoO <sub>x</sub> N <sub>y</sub>	76aN
Total indole conversion	93.3	63.5
Indole and N-containing compounds		
Indole	6.7	36.5
Indoline	3.2	15.2
Orthoethylaniline	45.2	15.25
Orthomethylaniline	9.3	7
Aniline	1.2	0.2
C4-aniline	0.1	0.0
Sum	65.7	74.1
Indole HDN products		
Ethylcyclohexane	15.9	14.6
Ethylcyclohexene	2.8	1.1
Ethylbenzene	6.2	1.6
C4-cyclohexane	0.4	0
C4-benzene	0.1	0
Sum	25.4	17.3
THQ cyclic compounds		
1-4 THQ	2.8	3.4
Orthopropylaniline	0.9	0.1
Propylbenzene	0.1	0.0
C3-cyclohexene	0.5	0
C3-cyclohexane	1	0.6
Sum	5.3	4.1
Dimers		
Sum	3.4	4.1
Total	99.8	99.6

compounds, whereas 25.4 mol% lead to HDN products following the routes 1 and 2 in Fig. 2. Two secondary reactions, involving acidic sites (enlargement of indoline to 1-4 THQ and dimerization), lead to 5.3 mol% of 1-4 THQ with all its HDN intermediates and products and 3.4 mol% of dimers. In the next section, a detailed analysis of each group of compounds will be given.

**3.3.1. Distribution of indole and N-containing compounds.** Table 2 shows all the intermediates of route 1 (Fig. 2). Indole hydrogenates to indoline (3.2 mol%), the latter of which undergoes a first C–N hydrogenolysis leading to OEA, the major intermediate product in the gas phase (45.2 mol%). Secondary C–C hydrogenolysis of the lateral alkyl chain of OEA can occur, leading to 9.3 mol% OMA and 1.2 mol% aniline. A very weak alkylation process produces butylaniline (C<sub>4</sub>-aniline) (0.1 mol%).

According to a “rake” mechanism (18), quasi-equilibria between compounds in the gas phase and their corresponding adsorbed species may be assumed. Only low concentrations of indole (6.7 mol%) and indoline (3.2 mol%) remain in the gas phase, showing that both molecules are transformed and, therefore, that the catalyst surface is mainly covered by adsorbed OEA, the major product in the gas phase.

**3.3.2. Distribution of indole HDN products.** Ethylcyclohexane, cyclohexene, and ethylbenzene are the main products. The two routes in Fig. 2 can be considered to be independent, taking into account that EB cannot transform to ECH in the presence of OEA because of the inhibiting effect of OEA, which strongly adsorbs on the surface. This behavior has already been described in previous studies of HDN on commercial catalysts (19, 20). In a parallel work, the same behavior was observed for bulk molybdenum oxynitrides: hydrogenation of propylbenzene (instead of EB) on MoO<sub>x</sub>N<sub>y</sub> decreased from 98 to 0% when orthopropylaniline (instead of OEA) was added to the feed at 543 K and 5 MPa. Therefore, the ratio (ECH + ECHE)/EB (18.7/6.2) = 3.0 permits the quantification of these two routes over MoN<sub>x</sub>O<sub>y</sub>.

Ethylcyclohexene (ECHE) (2.8 mol%) is the intermediate olefin between OECHA and ECH (Fig. 2), following a Hoffmann-type β-hydrogen elimination (21). At 600 K, hydrogenation is not sufficiently strong to completely transform ethylcyclohexene to ECH. Weak alkylations still occur and lead to 0.4 mol% butylcyclohexane and 0.1 mol% butylbenzene.

**3.3.3. Distribution of secondary products.** The main product observed is 1-4 THQ (2.8 mol%), due to the enlargement reaction of indoline. This enlargement requires the presence of surface acidic sites. All intermediates (OPA, propylcyclohexene (C<sub>3</sub>-CHene)), and products (ethylbenzene (EB), propylcyclohexane (PCH)) of the 1-4 THQ cycle were detected. Another active acidic site is also shown by the formation of dimers (3.4 mol%) (Table 2).

### 3.4. Comparison with Nitrated Supported Material (76 aN)

The detailed analysis of the intermediates and final products in the liquid phase resulting from the HDN of indole over 76aN was conducted in a similar manner as the analysis done over bulk MoO<sub>x</sub>N<sub>y</sub> (Table 2).

Table 2 (column 3) shows the lower global HDN activity of 76aN compared to MoO<sub>x</sub>N<sub>y</sub> (column 2) leading to a higher mol% of N-containing compounds (74.1 mol% instead of 65.7 mol%) and a lower mol% of products of HDN (17.3 mol% instead of 25.4 mol%).

In contrast, secondary reactions linked to the acidic function are quite similar. The lower HDN activity over 76aN appears in the intermediate distribution of indole and N-containing compounds. A higher amount of indole remains (36.5 mol% instead of 6.7 mol% for bulk MoO<sub>x</sub>N<sub>y</sub>), and a higher concentration of indoline (15.2 mol% instead of 3.2 mol%) is found; furthermore, the mol% of OEA is lowered by a factor of 3. Hydrogenolysis of the alkyl chain leading to orthomethylaniline (OMA) and aniline is also weaker.

For a lower HDN conversion of indole at 600 K, route 2 is favored on the supported material, as shown by the ratio (ECH + ECHE)/EB which is equal to (15.7/1.6) =

TABLE 3

**Distribution of Reaction Products and Intermediates (in mol%) Formed at 630 K and 9.1 MPa over MoO<sub>x</sub>N<sub>y</sub> and 76aN Catalysts**

Catalyst	MoO <sub>x</sub> N <sub>y</sub>	76aN
Total indole conversion	100	93.3
Indole and N-containing compounds		
Indole	0	6.7
Indoline	0	2.3
Orthoethylaniline	0.8	16.2
Orthomethylaniline	0.4	7.7
Aniline	0	0.6
C4-aniline	0	0
Sum	1.2	33.5
Indole HDN products		
Ethylcyclohexane	63.2	36.8
Ethylcyclohexene	1.2	1.1
Ethylbenzene	23.9	8.7
C4-cyclohexane	0.9	0.8
C4-benzene	0	0.1
Sum	89.2	47.5
THQ cyclic compounds		
1-4 THQ	0	0.3
Orthopropylaniline	0	0.6
Propylbenzene	0.4	0.6
C3-cyclohexene	0	0
C3-cyclohexane	5.8	5.8
Sum	6.2	7.3
Dimers		
Sum	3.2	11.3
Total	99.9	99.6

9.8 over 76aN instead of  $(18.7/6.2) = 3.0$  over MoO<sub>x</sub>N<sub>y</sub> (Table 2).

### 3.5. Effect of Temperature: HDN of Indole at 630 K over MoO<sub>x</sub>N<sub>y</sub>

Table 3 shows that products of the HDN of indole now represent 89.2 mol% of the total final liquid instead of 25.4 mol% at 600 K (Table 2, column 2), whereas only 1.2% of indole and N-containing compounds remain. In contrast, secondary reactions—enlargement of indoline to 1-4 THQ and its products of HDN (6.2 mol%) and dimers (3.2 mol%)—still remain in the same range as at 600 K: 6.2 mol% instead of 5.3 mol% at 600 K and 3.2 compared to 3.4 mol% at 600 K for dimers. This must be linked to a lower number of acidic sites or to fewer active acidic sites when the temperature is raised. This may also be due to a lower number of surface OH groups due to a reduction of the surface by H<sub>2</sub> at higher temperature.

Table 3 (column 2, first chemical group) shows that the higher HDN conversion observed corresponds to a total hydrogenation of indole to indoline and to a total C–N bond scission of the heterocycle of indoline to give mainly OEA + OMA. At 630 K, OEA is clearly the most abundant reactive intermediate, OMA corresponding again to a

C–C hydrogenolysis in accord with the metallic behavior of MoO<sub>x</sub>N<sub>y</sub> at this temperature.

Table 3 (column 2, second chemical group) shows the two major products of HDN: ethylbenzene (23.9 mol%) for route 1 and ethylcyclohexane (63.2 mol%) for route 2, with a ratio  $(ECH + ECHE)/EB (64.4/23.9) = 2.7$  corresponding to a high hydrogenating function.

### 3.6. Effect of Temperature: HDN of Indole at 630 K over 76aN

Table 3 (column 3) reports the detailed analysis of the intermediates and products over 76aN at 630 K. The moderate HDN activity (only 47.5 mol% of indole HDN products) is due to a moderate hydrogenating function as shown by the presence of unsaturated N-containing compounds.

In contrast, the activity of the acidic function of the support is enhanced when the reaction temperature is raised, leading to 7.3 mol% of 1-4 THQ cycle compounds and 11.3 mol% of dimers.

**3.6.1. Distribution of indole and N-containing compounds.** The low HDN activity and the low hydrogenating function are shown by the 6.7 mol% of indole that did not transform and the 2.3 mol% of indoline which still did not undergo C–N hydrogenolysis. OEA remains the major N-containing intermediate (16.2 mol%), leading to 7.7 mol% OMA by C–C bond scission. The same HDN elementary steps apply for both bulk and supported MoO<sub>x</sub>N<sub>y</sub>.

As a consequence of the moderate hydrogenating function of the 76aN material, 1.1 mol% of ethylcyclohexene still remains in the final liquid phase. Route 2 tends to be favored, as in the case of commercial sulfided NiMo/Al<sub>2</sub>O<sub>3</sub> catalysts, with  $(ECH + ECHE)/EB (37.9/8.7) = 4.4$  at 630 K (Table 3), instead of  $(ECH + ECHE)/EB (15.7/1.6) = 9.8$  at 600 K (Table 2).

**3.6.2. Comparison with bulk sample (MoO<sub>x</sub>N<sub>y</sub>).** The differences between bulk MoO<sub>x</sub>N<sub>y</sub> and 76aN materials in HDN activity, global hydrogenating, and metallic behavior, as well as the acidic function are now quite obvious from the data in Table 3.

In the presence of 70 ppm H<sub>2</sub>S, 33.5 mol% of indole and N-containing compounds still remain with the 76aN catalyst compared to only 1.2 mol% with the bulk material (Table 3, first chemical group).

The 76aN material presents only about 53% (47.5/89.2) of the total HDN activity of the bulk MoO<sub>x</sub>N<sub>y</sub> (Table 3, second chemical group).

Secondary reactions, occurring on acidic sites, lead to a higher hydroconversion of indoline to 1-4 THQ cyclic compounds and to a higher concentration of dimers (Table 3, third chemical group).

Data in Table 3 clearly show the large difference between the two catalysts: (i) MoO<sub>x</sub>N<sub>y</sub> gives practically no N-containing compounds (only low amounts of OEA and

OMA), whereas 76aN gives large amounts of all initial and intermediate compounds and (ii) different distributions of HDN products are observed where ECH + EB are the two major products for both materials.

### CONCLUSIONS

There are two ways to design new catalysts or new catalytic functions. The first is to prepare new materials (here the bulk  $\text{MoO}_x\text{N}_y$ ) or to modify existing catalysts (here a commercial NiMo-supported catalyst). In hydrotreating, NiMo-supported catalysts are generally sulfided to proceed to either the HDN or HDS reaction. The corresponding molybdenum sulfide can activate both  $\text{H}_2$  and the N-containing molecules. One of the main properties of sulfides, nitrides, and carbides is that they are able to exchange S, N, or C (7, 22). During HDN over a sulfided molybdenum catalyst, nitrogen insertion probably occurs. Oxynitrides and oxycarbides are efficient for activating dihydrogen and N-containing molecules. Thus, nitridation of a commercial NiMo-supported catalyst (76aN) can be achieved. Furthermore, bulk  $\text{MoO}_x\text{N}_y$  and 76a nitrided (76aN) present metallic and acidic functions. Since the 76aN material contains HZSM-5, its acidity is stronger. Sellem *et al.* (10) showed that, for  $\text{W}_2\text{N}/\text{EMT}$ , the nitridation step preserved the activity of the acid sites for isomerization and cracking.

One of the main results of this paper is that route 1 (Fig. 2) of the HDN of indole is possible over molybdenum oxynitride. This is in good agreement with the work of Abe and Bell (14), and Li and Lee (23) who performed HDN at low hydrogen pressure. A low hydrogen pressure does not thermodynamically favor hydrogenation, and these authors found a large amount of ethylbenzene, indicating the possibility of HDN via route 1, as described in our work. This route does not require the hydrogenating step of indole before C–N scission, and it is observed even under 9.1 MPa of hydrogen, as shown here.

### ACKNOWLEDGMENTS

This work was supported by the International Program for Scientific Cooperation, France–Poland, PICS 508, CNRS/ADEME/MAE, and by

the Action Concertée, France–Poland, the French Embassy, and the Polish Science Committee (KBN), Warsaw.

### REFERENCES

- Djéga-Mariadassou, G., Boudart, M., Bugli, G., and Sayag, C., *Catal. Lett.* **31**, 411 (1995).
- Ribeiro, F. H., Boudart, M., Dalla-Betta, R. A., and Iglesia, E., *J. Catal.* **130**, 498 (1991).
- Muller, A., Keller, V., Ducros, R., and Maire, G., *Catal. Lett.* **35**, 65 (1995).
- Sellem, S., Potvin, C., Manoli, J. M., Contant, R., and Djéga-Mariadassou, G., *J. Chem. Soc. Chem. Commun.*, 359 (1995).
- Volpe, L., and Boudart, M., *J. Solid State Chem.* **59**, 332 (1985).
- Ledoux, M. J., Guille, J., and Cuong, P. H., *J. Catal.* **194**, 176 (1988).
- Kim, H. S., Sayag, C., Bugli, G., Djéga-Mariadassou, G., and Boudart, M., *Mat. Res. Sci. Symp. Proc. Series* **368**, 3 (1995).
- Gouin, X., Marchand, R., L'Haridon, P., and Laurent, Y., *J. Solid State Chem.* **109**, 175 (1994).
- Sayag, C., Bugli, G., Havil, P., and Djéga-Mariadassou, G., *J. Catal.* **167**, 372 (1997).
- Sellem, S., Potvin, C., Manoli, J. M., Maquet, J., and Djéga-Mariadassou, G., *Catal. Lett.* **41**, 89 (1996).
- Bécue, T., Manoli, J. M., Potvin, C., and Djéga-Mariadassou, G., *J. Catal.* **170**, 123 (1997).
- Nagai, M., Kusagaya, T., Miyata, A., and Omi, S., *Bull. Soc. Chim. Belg.* **104**, Nos. 4–5 (1995).
- Kaernbach, W., Kisielow, W., Warzecha, L., Miga, K., and Klecan, R., *Fuel* **69**, 221 (1990).
- Abe, H., and Bell, A. T., *Catal. Lett.* **18**, 1 (1993).
- Bartholomew, C. H., Weatherbee, G. D., and Jarvi, G. A., *J. Catal.* **60**, 257 (1979).
- Breyse, M., Cattenot, M., Decamp, T., Frety, R., Gachet, C., Lacroix, M., Leclercq, C., de Mourgues, L., Portefaix, J. L., Vrinat, M., Houari, M., Grimblot, J., Kasztelan, S., Bonnelle, J. P., Housni, S., Bachelier, J., and Duchet, J. C., *Catal. Today* **4**, 39 (1988).
- Suzuki, M., Tsutsumi, K., Takahashi, H., and Saito, Y., *Zeolites* **9**, 98 (1989).
- Germain, J. E., "Catalytic Conversion of Hydrocarbons," p. 259. Academic Press, New York, 1969.
- Olivé, J. L., Biyoko, S., Moulinas, C., and Geneste, P., *Appl. Catal.* **19**, 165 (1985).
- Jian, M., Kapteijn, F., and Prins, R., *J. Catal.* **168**, 491 (1997).
- Perot, G., *Catal. Today* **10**, 447 (1991).
- Marchand, R. J., Gouin, X., Tessier, F., and Laurent, Y., *Proc. Mat. Res. Soc. Symp.* **368**, 15 (1994).
- Li, S., and Lee, J. S., *J. Catal.* **173**, 134 (1998).